Journal of Environmental Radioactivity 262 (2023) 107146

Contents lists available at ScienceDirect

Journal of Environmental Radioactivity

journal homepage: www.elsevier.com/locate/jenvrad

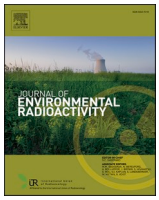

Generation of map on natural environmental background absorbed dose rate in India

Manish K. Mishra, S.K. Jha *, Aditi C. Patra, D.G. Mishra, S.K. Sahoo, S.K. Sahu, Gopal P. Verma, Shashank S. Saindane, Pratip Mitra, S. Garg, Vandana Pulhani, I.V. Saradhi, Probal Choudhury, A. Vinod Kumar, B.K. Sapra, M.S. Kulkarni, D.K. Aswal

Health, Safety and Environment Group, Bhabha Atomic Research Centre, Trombay, Mumbai, 400085, India

ARTICLE INFO

Handling Editor: Dr S.C. Sheppard

Keywords:
Natural background radiation
Primordial radionuclides
National map
Geographic information system
Absorbed dose rate

ABSTRACT

A systematic mapping of natural absorbed dose rate was carried out to assess the existing exposure situation in India. The mammoth nationwide survey covered the entire terrestrial region of the country comprising of 45127 sampling grids (grid size 36 km^2) with more than 100,000 data points. The data was processed using Geographic Information System. This study is based on established national and international approaches to provide linkage with conventional geochemical mapping of soil. Majority (93%) of the absorbed dose rate data was collected using handheld radiation survey meters and remaining were measured using environmental Thermo Luminescent Dosimeters. The mean absorbed dose rate of the entire country including several mineralized regions, was found to be 96 ± 21 nGy/h. The median, Geometric Mean and Geometric Standard Deviation values of absorbed dose rate were 94, 94 and 1.2 nGy/h, respectively. Among the High Background Radiation Areas of the country, absorbed dose rate varied from 700 to 9562 nGy/h in Karunagappally area of Kollam district, Kerala. The absorbed dose rate in the present nationwide study is comparable with the global database.

1. Introduction

Earth is surrounded by radiation of various kinds and intensities. Radiation arising from the decay of naturally occurring radionuclides along with cosmic radiation comprises natural background radiation at any location. Exposure to human being from natural resources is continuous and inescapable. In fact, the human race has evolved into its present form in the presence of background radiation (UNSCAER, 2000). The assessment of background gamma radiation dose from natural sources is of special interest considering the fact that it is the highest contributor to dose received by world population. Natural background radiation (NBR) can arise due to two major components, namely, external sources and internal sources. Sources include radioactivity in water, soil, food etc., which are incorporated in human body, building materials and the products that incorporate radioactive sources from nature. The main sources of natural background radiation are radioactive substances in the Earth's crust, emanation of radioactive gases from the Earth, cosmic radiation from outer space and trace amount of radioactivity in human body. The natural radiation from external sources varies by several orders of magnitude due to the variation in radioactive mineral content present in the lithosphere. The external component is divided into cosmic and terrestrial. The cosmic radiation is extraterrestrial in origin and generated by bombardment in the upper sphere of Earth by very high-energy alpha particles, protons, gamma rays, X-rays and other heavy charged particles. Terrestrial radiation is mainly emitted due to the presence of primordial radionuclides, with half-lives comparable to the age of the Earth, comprising of uranium, thorium, their daughter products and single radioisotopes like ^{40}K, ^{87}Rb, ^{147}Sm, ^{115}Ln, ^{138}La, ^{176}Lu etc. Inhalation exposure of the human population occurs primarily due to radon, thoron and their progeny. Radionuclides contributing to the dose to human population through the ingestion route are, primarily, ^{238}U, ^{232}Th series, their daughter products, and single isotopes like ^{40}K (UNSCEAR, 2000).

Rapid economic growth involves many human activities. Mining and milling of natural resources, extraction of petroleum products, use of ground water for domestic purposes and living in different types of houses alter the exposure levels. Naturally occurring radionuclides may be mobilized either by moving from inaccessible locations to areas where humans are present or concentrating the radionuclides present in the environment. In order to curb the global climate crisis, India has

* Corresponding author.
E-mail address: skjha@barc.gov.in (S.K. Jha).

https://doi.org/10.1016/j.jenvrad.2023.107146
Received 9 January 2023; Received in revised form 20 February 2023; Accepted 1 March 2023
Available online 8 March 2023

taken the pledge to achieve net zero CO_2 emission by 2070. In order to achieve this target, energy resources like nuclear, bio-fuel, green hydrogen, fuel cells etc. have to be tapped apart from coal. Since nuclear energy has least greenhouse gas emission potential; the interest in this energy sector has been renewed. The growth of the nuclear energy sector would also bring forth discussion associated with environmental levels of naturally occurring radioactive materials (NORMs). Hence, an up-to-date knowledge of the ambient background radiation prevailing in India is extremely important to alleviate public perception on radiation and its use. The objective of the present study is to generate a factual basis for public reference, present scientific research related to public exposure, exhibit spatial variation of natural air absorbed dose rate, study influence of radionuclide distribution in Earth's crust, create a basis for comparison in case of nuclear events and identification of mineralized metallogenic areas, granitic terrain etc. (Nambi et al., 1986; Sankaran et al., 1986; IAEA, 1990).

1.1. Approach for generation of national map

Gamma ray surveys have played an important role in systematic geochemical mapping since the past several decades (IAEA, 1990). The parameters that have an influence on the overall data quality in such surveys are: i) analytical technique, ii) instrument calibration, iii) quality control of generated data, and iv) variation due to geographical, geological and environmental conditions. Gamma surveys of environment may be handheld (on foot), airborne, vehicle-borne or by deploying environmental Thermo Luminescent dosimeters (TLDs), in boreholes, sea floor and in laboratories (IAEA, 1990; IAEA, 2003). Selection of the method adopted depends upon factors like, area of survey, analytical technique, equipment accessibility, resource availability etc. In airborne or vehicle-borne surveys gamma measurements are continuous and highly dense along the line of movement (IAEA, 1991). Ground based on-foot surveys, on the other hand, are point measurements at predefined sampling densities which correlate the ambient gamma levels with the radionuclide content in the A-horizon or upper regolith of soil. In general, it can be stated that the gamma surveys aim to provide radiometric data for all lithological units present in the study area (IAEA, 1990). Hence these surveys have been used to compile several regional and national radiometric maps (IAEA, 2003). Modern data processing tools have enabled new methods of data interpretation.

1.2. Scales of geological mapping

Representation of the ambient background radiation of a vast country like India requires efficient use of state-of the-art tools used in cartography. Contemporary cartography constitutes several practical and theoretical fundamentals of geographic information systems (GIS) and geographic information science (GISc). The cartographic scale is the ratio of distance on Earth compared to the same distance on a map. It can generally be described as local, regional or global. As evident by the terms, the maps constructed on the local scale are much more detailed compared to global maps. Local maps and regional maps generally identify anomalies in areas from few km^2 to tens or hundreds of km^2, respectively (Xuejing and Binchaun, 1993). In local scale, sampling is carried out in small grids in limited areas. In regional scale, the sampling interval widens. Geological maps in even larger areas of tens to millions of km^2 help in discovering geochemical provinces and mega-provinces. As evident, the density of sampling is lower in these surveys compared to regional surveys. This classification of geochemical patterns on spatial domains is essential to design a sampling programme for identifying specific geological areas (Xuejing and Binchaun, 1993).

Earlier study on national scale to construct the NBR map of India was carried out way back in 1986 (Nambi et al., 1986). The map was based on 214 sampling locations (data points). Considering the fact that India has a total area of 3.29 million km^2, the density of sampling locations was only or 6.6 per 1 lakh km^2. Hence, it was considered prudent to update the existing natural background radiation map of India with increased density of sampling locations, enhanced analytical capabilities and upgraded tools for data handling, interpretation, mapping and visualization. In the present study the updated and detailed natural background radiation map of India was generated using geographical information system (GIS).

2. Study area

India is a vast country housing diverse geological formations, natural resources (minerals, oil, forest and water), geographic features, landforms, soil characteristics and drainage pattern. It has rock formations and geological features ranging from primitive to the modern era. The stratigraphy of India can be classified into Archean, Dharwar, Cudappah, Vindhyan, Paleozoic, Mesozoic, Gondwana, Deccan Trap, Tertiary and Alluvial. The most primitive rocks of the Archean period are present in peninsular India and sedimentary rocks are housed in the Indo-Gangetic plains (Indian Minerals Yearbook, 2020; Ramakrishnan and Vaidyanadhan, 2008).

The geological formations may also be analyzed with the help of the geographical features. The physiographic divisions used for referencing Indian geological formations are, namely, the Himalayan Ranges, the Indo-Gangetic Plains, Extra Peninsular India, Peninsular India and Coastal sedimentary sequences (Indian Minerals Yearbook, 2020; Ramakrishnan and Vaidyanadhan, 2008).

3. Material and methods

India is a vast country having 3.29 million km^2 area with coastal, mountainous, forest, desert, riverine, plain and plateau regions. It was challenging to map the entire country due to uninhabited and inaccessible areas present in geologically diverse environments. Hence, to achieve the objective of nationwide monitoring, systematic and comprehensive field surveys were carried out on a nationwide scale.

Garmin, Etrex10, GPS system was used for providing latitude-longitude information (accurate within 12–20 m) of the sampling locations.

3.1. Grid size for absorbed dose rate measurements

Majority of absorbed dose rate measurements were carried out in a predetermined optimized grid size of 6 km × 6 km (36 km^2) throughout the country. Multiple measurements from a single grid were carried out near the approximate centre of each grid. The grid size was finalized after referring to similar studies and considering representativeness of the measured absorbed dose rate to the geological terrain (Xuejing and Binchaun, 1993).

The sampling locations covered in the present study on background absorbed dose rate are shown in Fig. 1 below. The absorbed dose rate was measured on a nationwide unified grid size of 36 km^2 covering all the states of India leaving the inaccessible and uninhabited regions.

A minimum sampling density of 1 sample/100 km^2 has been suggested by the International Geoscience Program, IGCP-259 report for national sampling programmes. In Estonia, Finland, Norway, Portugal, Romania, Slovenia and Sweden sampling densities of greater than 1 sample/100 km^2 have been followed. A number of studies (Gustavsson et al., 1994; Licht and Tarvainen, 1996) have combined sampling maps of different densities in Finland (1 sample/4 km^2), Sweden (1 sample/16 km^2) and Brazil (1sample/1 km^2). It is worth mentioning that the variation of sampling densities in Europe is wide, ranging from 1 sample/0.01 km^2 to 1 sample/3500 km^2.Similar methods of data presentation have also been used in UK successfully (Appleton, 1995). Most of the current geochemical maps have been produced using GIS and image-generating software (Gustavsson, 1994; Licht and Tarvainen, 1996). The quality of the final maps depends on several factors like density of sampling, tools for interpolation and final grid-size. Several

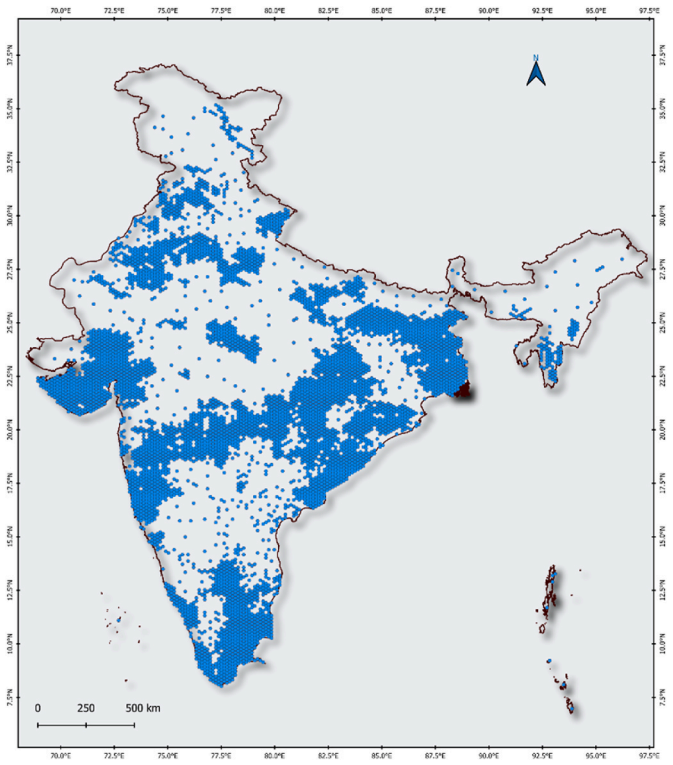

Fig. 1. Sampling locations for mapping of background absorbed dose rate in India.

authors (Fordyce et al., 1993; Garrett et al., 1990; Ridgway et al., 1991) have used averaging techniques to generate low density maps from high density of geochemical sampling data points.

Sampling stations were chosen in uncultivated lands and near population centres to account for various environmental factors involved in gamma radiation dose and to estimate public exposure. The survey meters calculated an average of 1 h absorbed dose rate based on multiple measurement results carried out at 1 m height above ground level. The results include both terrestrial and cosmic ray component of absorbed dose rate that was recorded in units of nGy/h.

3.2. Methodologies and instruments used for absorbed dose rate measurements

The gamma absorbed dose rate data has been generated mainly using three different instruments. The Geiger Muller Tube (GMT) based handheld radiation survey meters (Polimaster, model PM-1405) were used for most of the field measurements (93%) while TLDs were also used in some surveys. The NaI (Tl) based handheld detectors were also simultaneously used in few field surveys.

Thermo-luminescent Dosimeters (TLDs) are compact passive radiation dosimetry device used extensively worldwide for cumulative dose measurement (Goel and Murphy, 2020). Environmental TLDs were used for measurement of radiation exposure of the environment from terrestrial, cosmic and anthropogenic radiation present on the surface of the Earth. Details of the technique are given elsewhere (Karunakara et al., 2014).

In the present nationwide mapping, difficulties were faced in deployment of large number of TLDs in outdoor environment, limiting its use (Huang et al., 2016). Handheld survey meters, however, can be used to monitor absorbed dose rate of vast areas and, with proper automation, the data can be measured in real-time (GMT survey meters) or can be accumulated for a few seconds or minutes for getting time averaged absorbed dose rate.

Initial number of data points was around 100000. The data has been reduced by 'points-in-polygon' method of QGIS, by taking average of all the data-points in a single 36 km^2 grid. The following equation was used for calculation (QGIS, 2022).

$$Average\ doserate\ in\ a\ grid\ \left(\frac{nSv}{h}\right) = \frac{Sum\ of\ values\ of\ all\ the\ points\ in\ the\ grid}{Total\ number\ of\ points\ in\ the\ grid} \quad \text{Eq. 1}$$

Using this method, dense sampling data were reduced for a grid size of 36 km^2.

All radiation survey meters were calibrated at the calibration facility of BARC before carrying out any measurement. The radiation monitors have been calibrated using a ^{137}Cs source standardised as per ISO 4037 before deploying in the field conditions. All PM1405 monitors were calibrated at the calibration facility of BARC in terms of ADE (Ambient Dose Equivalent) before carrying out any measurement (Singh et al., 2023).

The ISO 4037 procedure was followed for the conversion of Sv to Gy. It may be noted that the factor of conversion from Gy to Sv ranges from 1.74 to 1 from 60 keV to 10 MeV. It varies in the range of 1.21 to 1.13 in the region of 662 keV to 3 MeV, which is the energy range in which most of the naturally occurring gamma energies occur. The highest naturally occurring gamma energy is 2614keV of ^{208}Tl (^{232}Th series) and 1764 keV of ^{214}Bi (^{238}U series). Considering the major gamma contribution from energies near 1.5 MeV, the conversion factor from Gy to Sv has been considered to be 1.15 (ISO 4037). Hence Sv to Gy conversion factor of 0.87 has been used in this study.

3.3. QA/QC of the instruments

All the systems/instruments used in survey were calibrated with a standard reference source at the calibration facilities of BARC which is the Designated Institute (DI) for ionizing radiation for various radiation levels and absorbed dose rate especially in the environmental range. Details of the calibration are given elsewhere (Saindane et al., 2018; Singh et al., 2023). Comparative assessment of GM Tube with NaI(Tl) crystal based detectors have been carried out by BARC, as a part of internal quality control exercises. A variation of <10% was observed between the two types of monitors. TLD and GM-tube based survey meter intercomparison was carried out by Karunakara et al. (2014). A good correlation was observed between the gamma dose rate values measured using TLD and portable survey meter. The agreement between the two techniques was observed to be good. The statistical uncertainty of the individual monitors was observed to be <10% (Chougaonkar et al., 2008).

3.4. Inverse Distance Weighted (IDW) interpolation for inaccessible locations

In QGIS, a geospatial interpolation method known as Inverse Distance Weighted (IDW), estimates the value at un-sampled locations using a combination of samples weighted by an inverse function of distance from the point of interest to the sampled points (Khouni et al., 2021). In principle, the samples closer to an un-sampled location have more influence than those located farther. A power factor (k) is used to control the weights. Greater values of '*k*' assign greater influence for the nearby points. IDW is a local exact interpolation technique. The general equation for IDW method is,

$$Z_a = \frac{\sum_{i=1}^{s} Z_i \times \frac{1}{d_j^k}}{\sum_{i=1}^{s} \frac{1}{d_j^k}} \quad \text{Eq. 2}$$

Where.

Z_a = estimated value at an unknown (un-sampled) location 'a'

Z_i = value at a control point 'i'
d_j = distance between sample point 'i' and location 'a'
s = number of sample points used in estimation (minimum 2)
k = power factor (a value 2 means inverse square, 3 mean inverse cube and so on)

The absorbed dose rate values also follow inverse square law and decrease rapidly when the detectors are moved away from the source of radiation. This phenomenon of reduction in absorbed dose rate with increase in distance from source was observed in the regions of HBRA in Kerala, where the absorbed dose rate values reduced to ambient background levels at a distance of hundreds of meters away from monazite beach sands. Globally, some studies have applied the IDW method for mapping of large areas (Cinelli et al., 2020).

3.5. Mapping, coordinate reference system and projection

The data was exported in comma separated values (csv) format to a geographical information system (QGIS ver. 3.26, ver.3.22 LTR) for geospatial processing and calculations. The coordinate reference system (CRS) used for the mapping was EPSG:4326-WGS 84, which is based on World Geodetic System 1984 ensemble with a limited accuracy of 2 m. The CRS uses latitude and longitude for coordinates (Lat/Long as geodetic alias) and for projection EPSG:3857 (WGS 84 pseudo-Mercator) which uses 'meter' as its unit (Brunner, 2013; ICAO, 2002; NOAA, 2022). We have used QGIS (QGIS Development Team, 2022) and R programing language R Studio for data analysis and statistics (R Core Team, 2013; RStudio Team, 2020).

4. Results and discussion

A total of 100000 absorbed dose rate data have been collected in this study under multiple sampling programmes. The data have been reduced to one representative sample in each 36 km^2 grid, resulting in 45127 data points. The data were then compiled, adequately compared for their biases, statistically evaluated and geospatially interpolated for calculation of absorbed dose rate levels for the entire country.

The central tendency of the distribution is given in Table 1 for different grid sizes of 36 km^2, 144 $km^2$and 2000 km^2 (after using IDW). The raw data was aggregated into larger areas of 144 $km^2$and 2000 km^2, with only one point representing the mean value of the grid. The grid size of 144 km^2 accommodated 4 square grids of 36 km^2. The four data points in the 144 km^2grid were then represented by a single data point for the 144 km^2 hexagonal grid. Similarly, the 2000 km^2 grids also represent multiple hexgrids. It may be mentioned here that local and regional geological maps are able to identify anomalies in areas covering tens of km^2 and hundreds of km^2, respectively (Xuejing and Binchaun, 1993). Global maps cover a larger area in thousands of km^2. Hence, in this study we have given a picture of the local, regional and global scenario of absorbed dose rate distribution in the country. Moreover, the initial data points received, as a result of various survey programmes, were not homogenous in geographical distribution due to many factors like inaccessibility, dense forest cover, extreme weather conditions, unavailability of commutation etc. The heterogeneous (non-representative) data points were harmonized by local averaging into uniform grid size of 36 km^2 for further data processing, aggregating and interpolating.

Table 1
Data aggregation from singular data points to larger areas using IDW method.

Parameter (nGy/h)	Grid 36 km^2 N = 45127	Hexgrid 144 km^2 N = 5596	IDW2000 km^2 N = 1816
Range (Maximum - Minimum)	20–550	21–530	39–250
Mean	113	110	96
Standard Deviation	48	41	21
Median	106	108	94
Geometric Mean	104	103	94
Geometric SD	1.5	1.5	1.2

N = number of samples.

From Table 1 it can be concluded that the aggregation to larger grid size (144 and 2000 km^2) reduces the influence of localized and regional lithogenic mineralisations, on the absorbed dose rate. The aggregation method not only reduced the data in a representative manner, i.e., keeping the overall structure of the distribution in similar form, but also removed the repetitive and dense data by local averaging. This aggregation technique has also been successfully applied in studies carried out globally (IAEA 1991; 2003).

To map the entire country, including inaccessible locations, the geospatial interpolation method of IDW was used. The benefits of using IDW method were several, including the generation of 704 missing data points and increasing the number of valid data points from 1112 to 1816. This kind of data aggregation to larger areas, however, can have two major implications. First, it hides the local variations in the absorbed dose rate. Such averaging may reduce the influence of higher absorbed dose rate values on the single value assumed for a grid. Secondly, lack of sufficient homogenous data in a region could attribute higher values to a larger geographical area. Hence in this manuscript we have provided the field data as well as aggregated data.

As can be seen from Table 1, the average absorbed dose rate for the country, for the 36 km^2, 144 km^2 and 2000 km^2 were 113 ± 48, 110 ± 41 and 96 ± 21 nGy/h, respectively. It can be observed that the largest grid size is associated with the minimum standard deviation due to the application of IDW method. Median absorbed dose rate changed from 106 to 94 nGy/h for grid sizes of 36 km^2 and 2000 km^2, respectively. This also corroborated the fact that median is the most robust measure of central tendency of a dataset. This change in median value is also reflected in the density distribution in Fig. 2 and Box-whisker plot shown in Fig. 3. Considering the 2000 km^2 grid size the GM and GSD of the dataset were 94 nGy/h and 1.2, respectively, which indicates similar trend of GM and median for different grid sizes.

From Fig. 2 it can be observed that the absorbed dose rate data tend towards a log-normal distribution. Hence the GM and GSD were used as the representatives of central tendency and dispersion of the data. The median being the robust representation of central tendency was also considered for the national average. It can be delineated from the figure that the kurtosis or 'peakedness' of the distribution increases as the grid size increases (2000 km^2 IDW absorbed dose rate). The distribution for 36 km^2, 144 km^2 and 2000 km^2 grid sizes show bimodal distribution of absorbed dose rate, with the lower modal value having greater probability of occurrence. It can also be noted that the two modes of the bimodal distributions are closely spaced, indicating that there is not wide variation in the corresponding absorbed dose rates. After application of IDW the distribution becomes predominantly unimodal with reduced dispersion of absorbed dose rate data. This is due to the inherent averaging nature of the IDW method. Also the mode after IDW lies in between the two modes of the other distributions, as seen in Fig. 2.

This is also evident from the Box plot shown in Fig. 3. From the Box plot (Fig. 3) it can be understood that the spread of data, number of outlier values and their influence are also affected by the aggregation technique. Histograms for absorbed dose rates have been given in Figs. 1 and 2 in supplementary information.

The national map of natural background absorbed dose rate of India is shown in Fig. 4. This map was generated using GIS tool and IDW method of data interpolation. Higher levels of absorbed dose rate were observed in the south-western tip of the country, along coastal Kerala and Tamil Nadu, in the central region of Telangana, coastal Andhra Pradesh and Odisha, in the North-eastern Meghalaya and in upper-northern part of Uttarakhand.

A national map with grid size of 144 km^2 has been included in Fig. 3 of supplementary information. Map of individual sampling points have also been indicated with geologically important areas in Fig. 4 of

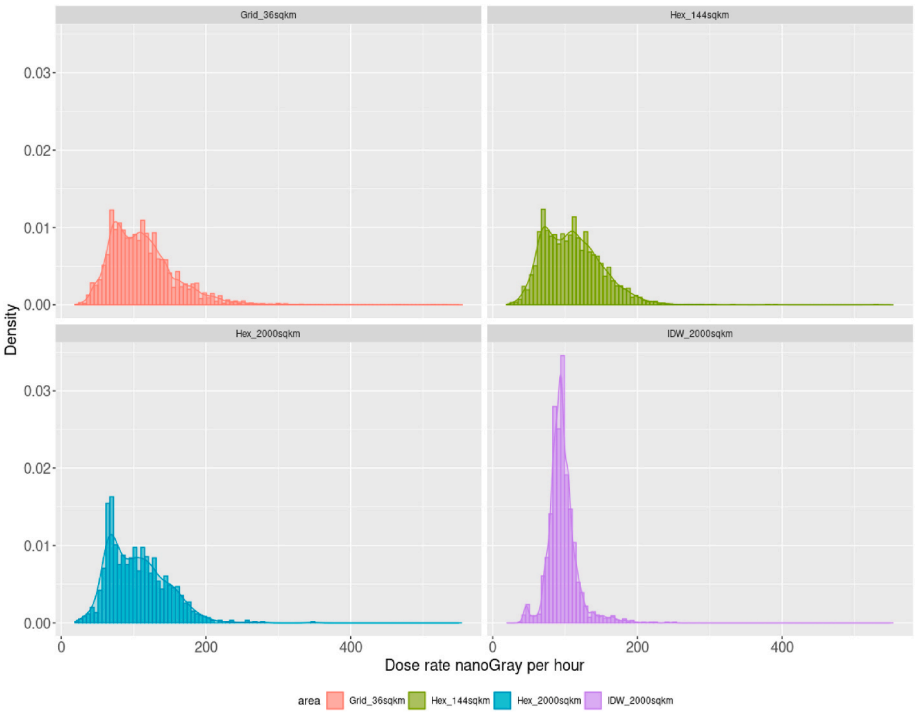

Fig. 2. A density distribution of the absorbed dose rate data after interpolation and acquiring the zonal statistics in (a) 36 km^2, (b) 144 km^2 and (c) 2000 km^2 hexagonal grids.

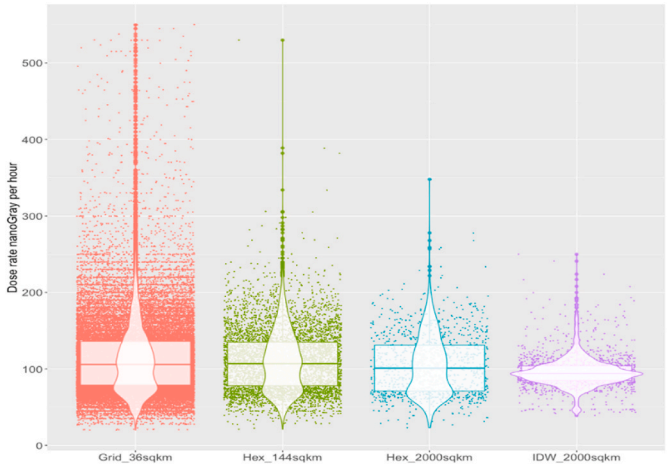

Fig. 3. Box plot of the data from 36 km^2, 144 km^2 and 2000 km^2 grid sizes.

supplementary information.

4.1. Variation of absorbed dose rate with the regional geology

The terrestrial gamma absorbed dose rate is primarily influenced by the regional geology. The absorbed dose rate values which were higher than 550 nGy/h, mainly found in the coastal Kerala with monazite deposition and a few locations in Eastern coast, were excluded from the calculation of the mean absorbed dose rate and were designated as HBRA (High Background Natural Radiation Areas) and treated separately. The map is provided in Supplementary Information Fig. 1.

Higher levels of absorbed dose rate in coastal southern Kerala and Tamil Nadu (700–9562 nGy/h in Karunagappally, Kollam, Kerala) are caused due to monazite placer deposits rich in thorium. The southern region of India in general has predominant presence of granitic rocks that serve as good geochemical hosts for U, Th and K (Sankaran et al., 1986).

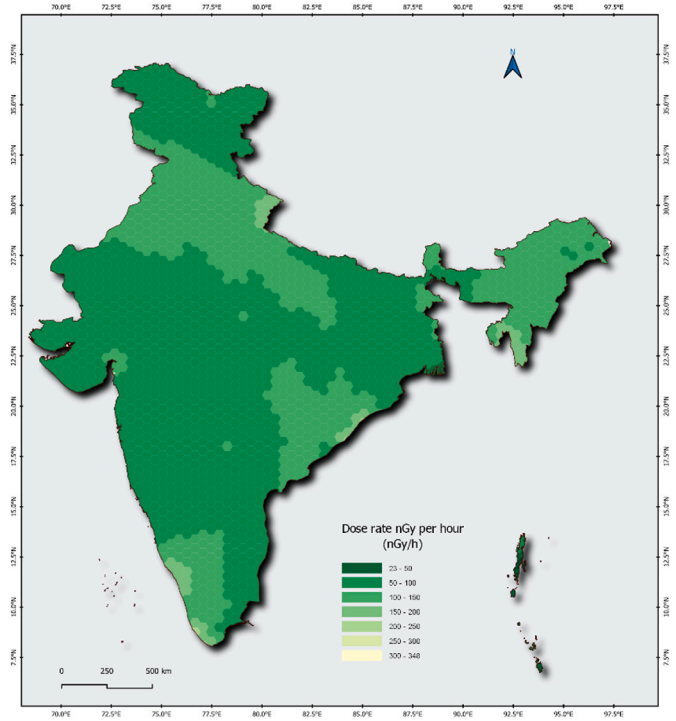

Fig. 4. Background gamma absorbed dose rate map of India generated using GIS and IDW method.

Studies by Sankaran (Sankaran et al., 1986) on external radiation dose to the population in India depict a wide range of ^{238}U in the soils. Their study revealed ^{238}U content of 1–3 ppm in the soils of Western India derived from Basalt rocks. The same has been observed in black soils obtained by weathering of trachy basalt or volcanic rocks with very

low ^{238}U content of around 0.6 ppm. The alluvial soils of Punjab composed of sediments of the Shivalik Hills and Himalayas carried by the rivers of Indus system are reported to contain uranium in the range of 0.4–5.9 ppm.

The part of central Telangana is also rich in granitic rock and gneisses raising the absorbed dose rate to the levels of ~290 nGy/h. The higher absorbed dose rate levels in Uttarakhand may be due to the higher contribution of the cosmic component at greater elevations as well as large scale granitic injections which took place in the Himalayas during Eocene-Miocene epochs (8–65 million years ago) (Sankaran et al., 1986). Some areas in North-eastern India also showed higher ambient gamma absorbed dose rates due to presence of natural mineralization (Sankaran et al., 1986; War et al., 2008).

We have found a slightly fair correlation between soil classes and absorbed dose rate. Low values (around 67 nGy/h) of absorbed dose rate in air were recorded for mixed red and black soils of Maharashtra and Gujarat while high values of (around 170 nGy/h) were recorded in the west-coastal plains of Kerala containing coastal and derived deltaic alluvial soils.

4.2. Comparison with earlier national database

The earlier national database was generated by Nambi (Nambi et al., 1986). In this study environmental TLDs were deployed on meteorological towers of Indian Meteorological Department (IMD) located at 214 locations throughout the country. The results of this study have been used till date for dose representation as well as calculation of dose to the public. The density of sampling locations was 6.6 samples per 1 lakh km^2, which is very low. Hence, in the present study a denser sampling density of 3.04 samples per 100 km^2 was generated. The average absorbed dose rate was reported as 89 ± 42 nGy/h by Nambi et al. Highest absorbed dose rate of 3002 nGy/h was observed at Chavara, Kerala. In the present study, the average, GM, median and GSD of absorbed dose rate were 96 ± 21, 94, 94 and 1.2 nGy/h. Highest dose of 9562 nGy/h was observed in Kollam, Kerala in the present national database. It is clear that denser sampling resulted in identification of newer areas or hotspots with substantially higher natural background absorbed dose rates. The benefit of a larger database is that several statistical parameters could also be derived from the data with greater confidence and the tools of aggregation and interpolation could be applied successfully. Hence, this study presents a national map of India which resolves and transforms the localized map of India generated earlier.

4.3. Comparison with global studies

The European Association has published an evidentiary document named 'European Atlas of Natural Radiation' which has been compiled from the data received from various countries in the Europe (Cinelli et al., 2020). In the United Kingdom study, a mean of 94.7 nGy/h (SD 15.6; range 38.1–159.7) was reported. This is comparable to present Indian average gamma absorbed dose rate of 94 nGy/h. The present study has also been compared with several other studies carried out globally and presented in Table 2 below. It can be seen that the absorbed dose rate obtained in the present nationwide study is comparable to several other countries.

Table 2
Comparison of current study with studies carried out globally.

Location	Absorbed dose rate in air (nGy/h)	Reference
Vietnam	75 ± 32	Inoue et al. (2020)
Central region, Ghana	100 ± 20	Faanu et al. (2016)
Southwest Nigeria	232	Jibiri et al. (2016)
Jos Plateau	250	Abba et al. (2017)
Malaysia	209	Nuraddeen et al. (2015)
Iran	105	Baykara and Dogru, 2009
Brazil	125	Freitas and Alencar (2004)
Minna, Nigeria	137	Shittu et al., 2021
Hassan, Korea	128	Hassan et al. (2018)
India	96 ± 21	Present study

5. Conclusion

The nationwide gamma absorbed dose rate map of India was revisited and updated after nearly four decades using new and improved techniques of measurement, data handling and visualization. Sampling density was increased from 6.6 samples per 1 lakh km^2 to 3.04 samples per 100 km^2 leading to a more well resolved data adopting a smaller sampling grid size of 36 km^2. In the present study, the average, GM, median and GSD of absorbed dose rate were 96 ± 21, 94, 94 and 1.2 nGy/h. Highest dose of 9562 nGy/h was observed in Kollam, Kerala in the present national database. Absorbed dose rate was observed to be high in certain areas of the country correlating well with underlying geological features like ancient shield, granites and sedimentary basins. This national absorbed dose rate map is going to have multifaceted uses and benefit the national and international scientific community and decision makers. Also, it comes at an opportune moment, when the nuclear programme of India is expanding at a faster pace in order to address the global climate change crisis.

Declaration of competing interest

The authors declare that they have no known competing financial interests or personal relationships that could have appeared to influence the work reported in this paper.

Data availability

The authors are unable or have chosen not to specify which data has been used.

Acknowledgements

We acknowledge the help, support and hard work of the employees and field staff of HS&EG, BARC spread all over the country who have been instrumental in providing technical support for collection of the enormous set of data.

Appendix A. Supplementary data

Supplementary data to this article can be found online at https://doi.org/10.1016/j.jenvrad.2023.107146.

References

Abba, H.T., Saleh, M.A., Hassan, W.M.S.W., Aliyu, A., Ramli, A.T., 2017. Mapping of natural gamma radiation (NGR) dose rate distribution in tin mining areas of Jos Plateau, Nigeria. Environ. Earth Sci. 76, 208. https://doi.org/10.1007/s12665-017-6534-8.

Appleton, J.D., 1995. Potentially Harmful Elements from Natural Sources and Mining Areas: Characteristics, Extent and Relevance to Planning and Development in Great Britain, 95/3. British Geological Survey Technical Report WP, Keyworth.

Baykara O and Dogru M. Determination of terrestrial gamma, 2009. ^{238} U, ^{232} Th and ^{40} K in soil along fracture zones. Radiat. Meas., 44: 116–121.

Brunner, F.K., 2013. Advances in Positioning and Reference Frames: IAG Scientific Assembly Rio de Janeiro, Brazil, September 3–9, 1997. Springer Science & Business Media.

Chougaonkar, M.P., Takale, R.A., Shetty, P.G., Mayya, Y.S., 2008. Performance Characteristics of $CaSO_4$:Dy Based Indigenous Thermoluminescent Dosimeters for Environmental Radiation Monitoring. BARC/2008/E/007.

Cinelli, G., De, C.M., Tollefsen, T., Achatz, M., Ajtić, J., Ballabio, C., Barnet, I., Bochicchio, F., Borelli, P., Bossew, P., Braga, R., Brattich, E., Briganti, A., Carpentieri, C., Castellani, C.-M., Castelluccio, M., Chiaberto, E., Ciotoli, G.,

Coletti, C., Zhukovsky, M., 2020. European Atlas of Natural Radiation. JRC Publications Repository. https://doi.org/10.2760/46388.
Faanu, A., Adukpo, O.K., Kansaana, C., Tettey-Larbi, L., Lawluvi, H., Kpeglo, D.O., 2016. Impact assessment of naturally occurring radioactive materials on the public from gold mining and processing at Newmont Golden Ridge Limited, Akyem, Eastern Region of Ghana. Radiat. Protect. Environ. 39, 155–164.
Fordyce, F.M., Green, P.M., Simpson, P.R., 1993. Simulation of regional geochemical survey maps at variable sample density. J. Geochem. Explor. 49, 161–175.
Freitas, A., Alencar, A., 2004. Gamma dose rates and distribution of natural radionuclides in sand beaches–Ilha Grande, Southeastern Brazil. J. Environ. Radioact. 75, 211–223.
Garrett, R.G., Banville, R.M.P., Adcock, S.W., 1990. Regional geochemical data compilation and map presentation, Labrador, Canada. J. Geochem. Explor. 39 (1/2), 91–117.
Goel, A., Murphy, A., 2020. Thermoluminescent Dosimeter-Radiology Reference Article. Radiopaedia.Org. https://radiopaedia.org/articles/thermoluminescent-dosimeter?lang=us.
Gustavsson, N., Lampio, E., Nilsson, B., Norblad, G., Ros, F., Salminen, R., 1994. Geochemical maps of Finland and Sweden. J. Geochem. Explor. 51, 143–160.
Hassan, N.M., Kim, Y.J., Jang, J., Chang, B.U., Chae, J.S., 2018. Comparative study of precise measurements of natural radionuclides and radiation dose using in-situ and laboratory γ-ray spectroscopy techniques. Sci. Rep. 8 (1), 1–11.
Huang, Y.-J., Guo, G.-Y., He, Y., Yang, L.-T., Shan, Z., Chen, C.-F., Shang-Guan, Z.-H., 2016. A comparative study of terrestrial gamma absorbed dose rate in air measured by thermoluminescent dosimeter, portable survey meter and HPGe gamma spectrometer. J. Environ. Radioact. 164, 13–18. https://doi.org/10.1016/j.jenvrad.2016.06.020.
IAEA, 1990. The Use of Gamma Ray Data to Define Natural Radiation Environment. IAEA-TECDOC-566. IAEA, Vienna.
IAEA, 1991. Airborne Gamma ray spectrometer surveying. IARA-TRS-323. IAEA-TECDOC-566, ISSN 0074-1914. IAEA, Vienna, pp. 53-93, May 1991.
IAEA, 2003. Guidelines for Radioelement Mapping Using Gamma Ray Spectrometry Data. IAEA-TECDOC-1363. IAEA, Vienna.
ICAO, 2002. World geodetic system-1984 (WGS-84) manual (international civil aviation organisation). In: International Civil Aviation Organisation. https://www.icao.int/NACC/Documents/Meetings/2014/ECARAIM/REF08-Doc9674.pdf.
Indian Minerals Yearbook 2020, 2021. Government of India, Ministry of Mines. Indian Bureau of mines.
Inoue, K., Fukushi, M., Van Le, T., 2020. Distribution of gamma radiation dose rate related with natural radionuclides in all of Vietnam and radiological risk assessment of the built-up environment. Sci. Rep. 10, 12428 https://doi.org/10.1038/s41598-020-69003-0.
Jibiri, N., Isinkaye, M., Bello, I., Olaniyi, P., 2016. Dose assessments from the measured radioactivity in soil, rock, clay, sediment and food crop samples of an elevated radiation area in south-western Nigeria. Environ. Earth Sci. 75, 107.
Karunakara, N., Yashodhara, I., Sudeep Kumara, K., Tripathi, R.M., Menon, S.N., Kadam, S., Chougaonkar, M.P., 2014. Assessment of ambient gamma absorbed dose rate around a prospective uranium mining area of South India – a comparative study of dose by direct methods and soil radioactivity measurements. Results Phys. 4, 20–27.
Khouni, I., Louhichi, G., Ghrabi, A., 2021. Use of GIS based inverse distance weighted interpolation to assess surface water quality: case of wadi el bey, Tunisia. Environ. Technol. Innovat. 24, 101892 https://doi.org/10.1016/j.eti.2021.101892.
Licht, O.A.B., Tarvainen, T., 1996. Multipurpose geochemical maps produced by integration of geochemical exploration datasets in the Parana Shield, Brazil. J. Geochem. Explor. 55 (3), 167–182.
Nambi, K.S.V., Bapat, V.N., David, M., Sundaram, V.K., Sunta, C.M., 1986. Natural background radiation and population dose distribution in India. Bhabha Atomic Research Centre. INS 20 (24), 900696.
NOAA, 2022. Chapter 8: the World Geodetic System. National Oceanic and Atmospheric Administration, Geodesy. https://geodesy.noaa.gov/PUBS_LIB/Geodesy4Layman/TR80003E.HTM.
Nuraddeen, N.G., Ahmad, T.R., Muneer, A.S., Syazwan, M.S., Hamman, T.G., 2015. Radiological mapping of Kelantan, Malaysia using terrestrial radiation dose rate. Isot. Environ. Health Stud. https://doi.org/10.1080/10256016.2016.1095189.
QGIS Development Team, 2022. QGIS Geographic Information System. QGIS Association. https://www.qgis.org.
R Core Team, 2013. R: A Language and Environment for Statistical Computing. R Foundation for Statistical Computing. http://www.R-project.org/.
Ramakrishnan, M., Vaidyanadhan, R., 2008. Geol. India 1 and 2. No: 978-81-85867-98-4, Geological Society of India.
Ridgway, J., Appleton, J.D., Greally, K.B., 1991. Variations in regional geochemical patterns, effects of site-selection and data-processing algorithms. Trans. Inst. Min. Metall. 100, 122–130.
RStudio Team, 2020. RStudio: integrated development environment for R. RStudio, PBC. http://www.rstudio.com/.
Saindane, S.S., Narsaiah, M.V.R., Pujari, R.N., Murali, S., Kumar, A.V., 2018. Use of Mobile Monitoting Techniques for Radiological Aspects in Nuclear Industry. Raja Ramanna Centre for Advance Technology.
Sankaran, A.V., Jayaswal, B., Nambi, K.S.V., Sunta, C.M., 1986. U, Th and K Distributions Inferred from Regional Geology and the Terrestrial Radiation Profiles in India. SIRD Bhabha Atomic Research Centre.
Shittu, H.O., Olarinoye, I.O., Kolo, M.T., Amadi, A.N., Olukotun, S.F., Oladejo, O.F., Samuel, G.E.K., 2021. Mapping of natural gamma radiation (NGR) dose rate distribution around gidan-kwano area, minna, North-Central Nigeria. FUW Trend Sci. Technol. J. 6 (3), 931–936.
Singh, S.K., Shaiju, L., Sathian, V., Chaudhury, P., 2023. Establishment of a facility for calibration of low level gamma radiation monitors: a preliminary study. Proceedings of 6th Asian and Oceanic Congress for Radiation Protection, 07-11 Feb 2023. Radiat Prot. Environ. Feb. 46 (5), 151–153. https://doi.org/10.4103/0972-0464.368742.
UNSCEAR, 2000. Sources and Effects of Ionizing Radiation: United Nations Scientific Committee on the Effects of Atomic radiation UNSCEAR 2000 Report, 1. United Nations General Assembly, New York.
War, S.A., Nongkynrih, P., Khathing, D.T., Iongwai, P.S., Jha, S.K., 2008. Spatial distribution of natural radioactivity levels in topsoil around the high-uranium mineralization zone of Kylleng-Pyndensohiong (Mawthabah) areas, West Khasi Hills District, Meghalaya, India. J. Environ. Radioact. 99 (10), 1665–1670.
Xuejing, X., Binchaun, Y., 1993. Geochemical patterns from local to global. J. Geochem. Explor. 47, 109–129.